View Article Online / Journal Homepage / Table of Contents for this issue

A new class of "all-metal" aromatic hydrido-bridged binary coinage metal heterocycles. A DFT study†

Athanassios C. Tsipis* and Alexandros V. Stalikas

Received (in Durham, UK) 23rd November 2006, Accepted 21st March 2007
First published as an Advance Article on the web 3rd April 2007
DOI: 10.1039/b617158c

Published on 03 April 2007 on http://pubs.rsc.org | doi:10.1039/B617158C
Downloaded by University of Belgrade on 01 January 2013

Electronic structure calculations (DFT) suggest that the series of hydrido-bridged binary coinage metal clusters with general formulae *cyclo*-$Cu_nAg_{3-n}(\mu_2\text{-}H)_n$ (n = 1–3), *cyclo*-$Cu_nAg_{4-n}(\mu_2\text{-}H)_n$ (n = 1–4) and *cyclo*-$Cu_nAg_{5-n}(\mu_2\text{-}H)_n$ (n = 1–5) are stable entities. The aromaticity of these bimetallic systems was explored by employing a number of established criteria such as the nucleus-independent chemical shift, the hardness, η, and the electrophilicity index, ω. Aromaticity decreases upon increasing the number of Cu atoms in the metallic ring core structure or increasing its size. The structural, energetic, spectroscopic (IR, NMR, UV-Vis) and electronic properties of these novel classes of inorganic compounds characterized by a common ring-shaped electron density are thoroughly analyzed. The hydrido-bridged binary coinage metal clusters exhibit a composite bonding mode involving both σ-, π- and δ-type components. Noteworthy is the presence of π-type MOs resulting from the bonding interaction of *n*d AOs of the metal atoms, delocalized over the entire metallic framework analogous to the π-type MOs of the aromatic hydrocarbons.

1. Introduction

Coinage metals have a strong tendency to cluster together forming a wide variety of cyclic polynuclear complexes with metal–metal distances shorter than the sum of their van der Waals radii.[1] Copper(I) centers form a large variety of organocopper(I) compounds[2–4] bearing a cyclic polynuclear metal core, the most representative example being the cyclic Cu_4R_4 tetramers (R = alkyl).[5] The same holds also true for the other two congeners *e.g.* Ag(I) and Au(I). A vast number of organosilver(I) and organogold(I) compounds formulated as M_nL_n (M = Ag or Au; L = bridging ligand) has been reported so far.[6–8] The cyclic polynuclear coinage metal clusters are characterized by perfect planarity of their core metallic ring structure as well as by high stability.

Attractive d^{10}–d^{10} bonding interactions seem to support the self-association of the Cu(I), Ag(I) and Au(I) complexes to form three-, four- and five-membered metal rings and the terms cuprophilicity, argentophilicity and aurophilicity have been used to describe these closed-shell metal–metal interactions.[9–12] However, we have recently demonstrated that a series of hydrido-bridged planar cyclic hydrocopper(I),[13] hydrosilver(I) and hydrogold(I)[14] analogues of aromatic hydrocarbons are aromatic molecules characterized by a common ring-shaped electron density involving σ-, π- and δ-type delocalization of the transition metal d-electrons. A quantitative evidence of d-orbital aromaticity in square-planar coinage metal clusters was provided by Schleyer *et al.*[15,16] These findings expand the concept of aromaticity, more commonly seen for organic molecules, to the realm of all-metal systems[17,18] with structures resembling those of the aromatic hydrocarbons. The fascinating properties of such systems span not only the concepts of metalloaromaticity and metallophilic bonding but also other fundamental areas such as acid–base chemistry, supramolecular assemblies, M–M-bonded excimers, host–guest chemistry, luminescence, *etc.*[19] Surprisingly, cyclic polynuclear complexes containing the Cu–Ag interaction are very rare whereas M–M (M = Cu, Ag or Au), Cu–Au and Ag–Au interactions are very common.[20]

In this context, we address here a number of important issues related to the molecular and electronic structures, stabilities, bonding features, and spectroscopic properties of a series of hydrido-bridged binary coinage metal clusters with general formulae *cyclo*-$Cu_nAg_{3-n}(\mu_2\text{-}H)_n$ (n = 1–3), *cyclo*-$Cu_nAg_{4-n}(\mu_2\text{-}H)_n$ (n = 1–4) and *cyclo*-$Cu_nAg_{5-n}(\mu_2\text{-}H)_n$ (n = 1–5).

2. Computational details

The structural, electronic, and energetic properties of all compounds were computed with Becke's three parameter hybrid functional[21,22] combined with the Lee–Yang–Parr correlation functional,[23] abbreviated as B3LYP, using the LANL2DZ basis set for Ag atom and the 6-31G(d,p) for all other atoms. In all computations no constraints were imposed on the geometry. Full geometry optimization was performed for each structure using Schlegel's analytical gradient method[24] and the attainment of the energy minimum was verified by calculating the vibrational frequencies that result in absence of imaginary eigenvalues. The natural bond orbital (NBO) population analysis was performed using Weinhold's methodology.[25,26] Magnetic shielding tensors have been computed

Laboratory of Inorganic Chemistry, Department of Chemistry, University of Ioannina, 451 10 Ioannina, Greece. E-mail: attsipis@cc.uoi.gr; Fax: +30 26510 98409; Tel: +30 26510 98333

† Electronic supplementary information (ESI) available: MOs, structures and IR data for the species discussed. See DOI: 10.1039/b617158c

 This journal is © the Royal Society of Chemistry and the Centre National de la Recherche Scientifique 2007

Published on 03 April 2007 on http://pubs.rsc.org | doi:10.1039/B617158C
Downloaded by University of Belgrade on 01 January 2013

with the GIAO (gauge-including atomic orbitals) method,[27,28] as implemented in the GAUSSIAN03 series of programs employing the B3LYP level of theory. Nucleus independent chemical shift (NICS) values were computed at the B3LYP/LANL2DZ level according to the procedure described by Schleyer *et al.*[29] The magnetic shielding tensor element was calculated for a host atom located at the center of the ring. Time-dependent density functional theory (TD-DFT)[30–32] calculations were performed on the equilibrium ground-state geometries employing the same density functionals and basis sets used in geometry optimization. All calculations were performed using the GAUSSIAN03 suite of programs.[33]

3. Results and discussion

3.1 Equilibrium geometries

The equilibrium geometries of the hydrido-bridged binary coinage metal clusters, *cyclo*-$Cu_nAg_{3-n}(\mu_2\text{-H})_n$ (n = 1–3), *cyclo*-$Cu_nAg_{4-n}(\mu_2\text{-H})_n$ (n = 1–4) and *cyclo*-$Cu_nAg_{5-n}(\mu_2\text{-H})_n$ (n = 1–5) are given in Fig. 1, 2 and 3, respectively.

It can be seen that the cyclic trinuclear and tetranuclear hydrometals adopt a perfect planar configuration. The triangular core structures of the parent hydrido-bridged homonuclear, *cyclo*-$Cu_3(\mu_2\text{-H})_3$, **1** and *cyclo*-$Ag_3(\mu_2\text{-H})_3$, **4**, species correspond to perfect equilateral triangles, while those of the heteronuclear *cyclo*-$Cu_2Ag(\mu_2\text{-H})_3$, **2** and *cyclo*-$CuAg_2(\mu_2\text{-H})_3$, **3**, ones to isosceles triangles. The 4-membered all-metal ring structural core in the homonuclear *cyclo*-$Cu_4(\mu_2\text{-H})_4$, **5** and *cyclo*-$Ag_4(\mu_2\text{-H})_4$, **10**, species corresponds to a perfect square, while in the heteronuclear species **6–9**, adopts a diamond-shaped rhombic geometry. Finally, in the pentanuclear clusters the five metal ring atoms are coplanar forming a perfectly planar 5-membered metallic ring core structure. Exceptions are compounds **11**, **12** and **13** where the RMS deviation (root mean square deviation from a least squares plane fitted to the five metal atoms of the ring) is 0.069, 0.063 and 0.055 Å, respectively. The RMS deviation vanishes upon increasing the number of silver(I) atoms in the metallic ring. The computed metal–metal, M–M distances were found in the range of 2.773–2.858 Å, 2.370–2.509 Å and 2.581–2.693 for Ag–Ag, Cu–Cu and Cu–Ag bonds, respectively. The Cu–Cu, Ag–Ag and Cu–Ag distances are less than those expected by the sum of the van der Waals radii for Cu and Ag (280.0 pm and 344.0 pm, respectively).[34] The computed Cu–H and Ag–H bond lengths of the hydrido-bridges found in the regions of 1.600–1.672 Å and 1.784–1.944 Å, respectively, decrease when going from the three- to the five-membered all-metal rings.

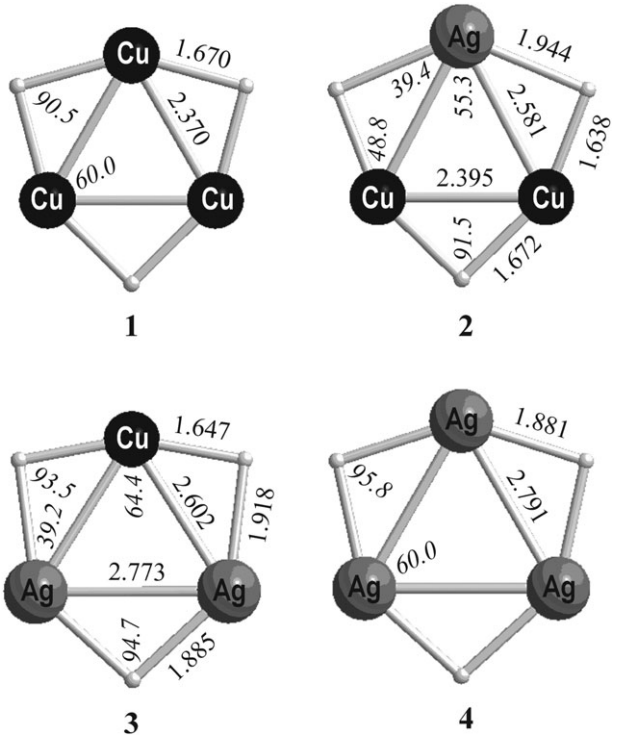

Fig. 1 Equilibrium geometries of the *cyclo*-$Cu_nAg_{3-n}(\mu_2\text{-H})_n$ (n = 1–3) metal clusters computed at the B3LYP/6-31G(d,p) ∪ LANL2DZ(Ag) level.

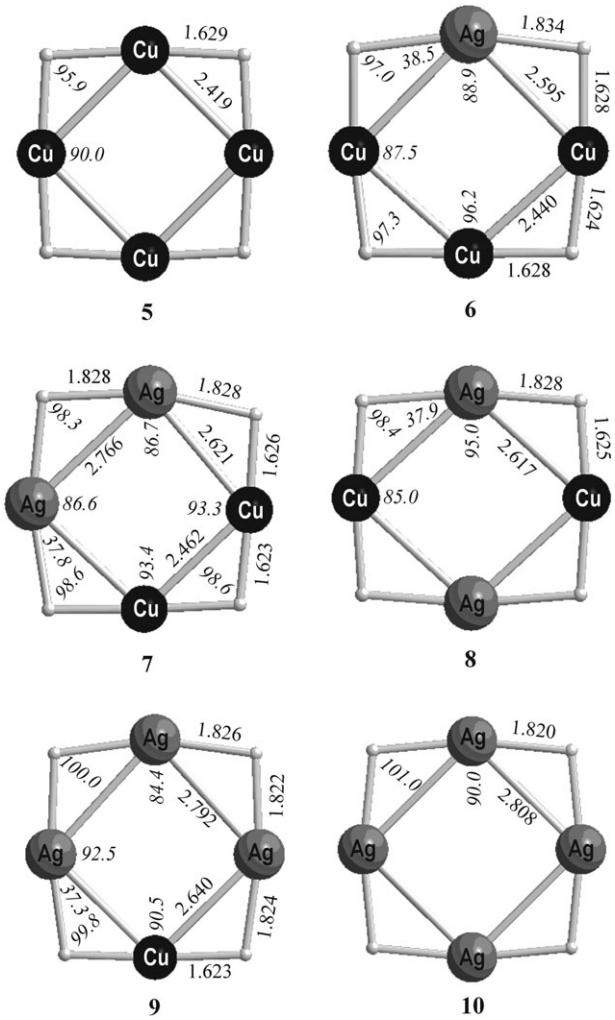

Fig. 2 Equilibrium geometries of the metal clusters, *cyclo*-$Cu_nAg_{4-n}(\mu_2\text{-H})_n$ (n = 1–4) metal clusters computed at the B3LYP/6-31G(d,p) ∪ LANL2DZ(Ag) level.

Published on 03 April 2007 on http://pubs.rsc.org | doi:10.1039/B617158C
Downloaded by University of Belgrade on 01 January 2013

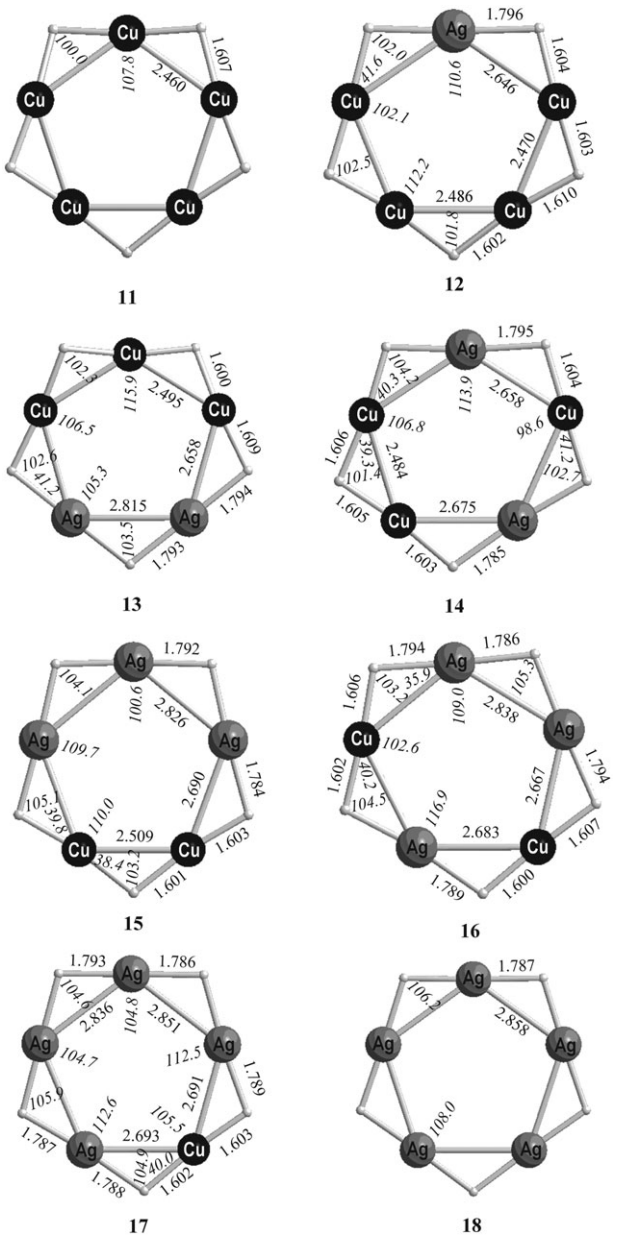

Fig. 3 Equilibrium geometries of the *cyclo*-$Cu_nAg_{5-n}(\mu_2\text{-}H)_n$ (n = 1–5) metal clusters computed at the B3LYP/6-31G(d,p) ∪ LANL2DZ(Ag) level.

3.2 Stability

The stability of the cyclic hydrometals is examined with respect to their dissociation to (i) MH monomers, (ii) free M and H atoms in their ground states, and (iii) the standard states of their elements, *e.g.* M and H_2. The calculated binding energies are given in Table 1.

It can be seen that all cyclic hydrometals are predicted to be bound with respect to their dissociation either to the MH monomers or to free M and H atoms in their ground states. Such strong interactions (ΔE_1/MH = 21–69 kcal mol^{-1}) could not be accounted for by the weaker metallophilic interactions (amounted to 7–12 kcal mol^{-1}).[10] Thereby it is the cyclic electron density delocalization over the "all-metal" aromatic ring that stabilizes the cyclic hydrometals. Moreover, the formation of the hydrido-bridged binary coinage metal clusters from their elements M(s) and H_2(g) corresponds to an exothermic process. The computed exothermicities, found in the range of −55.2 to −260.3 kcal mol^{-1}, increase upon increasing the number of Cu(I) atoms in the metallic ring core structure. Thus, the computed exothermicity for the formation of the *cyclo*-$Cu_5(\mu_2\text{-}H)_5$, 11 species is −260.3 kcal mol^{-1}, while that for the corresponding silver(I) analogue, *cyclo*-$Ag_5(\mu_2\text{-}H)_5$, **18**, amounts to only −143.6 kcal mol^{-1}.

3.3 Electronic and bonding properties

The most relevant molecular orbitals of the *cyclo*-$Cu_nAg_{3-n}(\mu_2\text{-}H)_n$ (n = 1–3) species are given in Fig. 4. The corresponding MOs of the *cyclo*-$Cu_nAg_{4-n}(\mu_2\text{-}H)_n$ (n = 1–4) and *cyclo*-$Cu_nAg_{5-n}(\mu_2\text{-}H)_n$ (n = 1–5) species are given in Fig. S1 and S2, respectively in the ESI.†

Perusal of Fig. 4 reveals that the metallacycle ring core structures exhibit a composite bonding mode involving σ-, π-, and δ-type components. It is important to be noticed that in the homonuclear species **1** and **4**, there exist highly delocalized over the entire metallic ring, *e.g.* HOMO-2 and HOMO-8 (δ-MOs), HOMO-13 (π-MO) and HOMO-14 (σ-MO), resulting from bonding interactions of the appropriate (n − 1)d AOs of the ring metal atoms. In addition, a highly delocalized σ-MO (HOMO-26) is constructed from the in-phase interactions between the np AOs of the ring metal atoms (npσ–npσ interactions). In the heteronuclear species **2** and **3**, the HOMO-13 (π-MO)—resulting from ndπ–ndπ bonding interactions—is mainly localized on the Ag(I) atoms of the metallic ring. Analogous, highly delocalized over the entire metallic ring, MOs are also observed in the tetranuclear and pentanuclear clusters, *cyclo*-$Cu_nAg_{4-n}(\mu_2\text{-}H)_n$ (n = 1–4) and *cyclo*-$Cu_nAg_{5-n}(\mu_2\text{-}H)_n$ (n = 1–5) (Fig. S1 and S2†). The cyclic delocalization of the electron density which supports a ring current is reminiscent of aromaticity, usually observed for aromatic hydrocarbons.

The stability of the hydrido-bridged binary coinage metal heterocycles is also reflected on the large HOMO–LUMO energy gap, $\varepsilon_{(lumo-homo)}$ (Table 2). According to the computed HOMO–LUMO energy gap the most stable species are predicted to be the 5-membered metallic ring followed by the 4- and 3-membered rings. Moreover, the heteronuclear metal ring core structures are predicted to be less stable than the homonuclear ones. The extent of aromaticity of the hydrido-bridged binary coinage metal heterocycles is also reflected on the electrophilicity index ω values (Table 2) given by the equation[35] $\omega = \mu^2/2\eta$, where η is the hardness and μ the chemical potential calculated by the expressions $(\varepsilon_{LUMO} - \varepsilon_{HOMO})/2$ and $(\varepsilon_{LUMO} + \varepsilon_{HOMO})/2$, respectively. The electrophilicity index ω is considered to be a measure of the electrophilic character of a molecule. Finally, no significant differences could be observed in the values of the electronic chemical potential, μ, which is considered as the opposite of the electronegativity, χ ($\mu = -\chi$).[36] It is worth to be noticed that the computed values for ω, η or μ do not follow any specific trend relative to the size or the nature of the species **1–18**.

 This journal is © the Royal Society of Chemistry and the Centre National de la Recherche Scientifique 2007

Published on 03 April 2007 on http://pubs.rsc.org | doi:10.1039/B617158C
Downloaded by University of Belgrade on 01 January 2013

Table 1 Binding energies ΔE_1, ΔE_2, and ΔE_3 of the *cyclo*-$Cu_nAg_{3-n}(\mu_2\text{-H})_n$ (n = 1–3), *cyclo*-$Cu_nAg_{4-n}(\mu_2\text{-H})_n$ (n = 1–4) and *cyclo*-$Cu_nAg_{5-n}(\mu_2\text{-H})_n$ (n = 1–5), calculated at the B3LYP/6-31G(d,p) ∪ LANL2DZ(Ag) level

Species	ΔE_1[a]/kcal mol^{-1}	ΔE_2[b]/kcal mol^{-1}	ΔH_3[c]/kcal mol^{-1}
cyclo-$Cu_3(\mu_2\text{-H})_3$ **1**	–95.5	–293.7	–126.7
cyclo-$Cu_2Ag(\mu_2\text{-H})_3$ **2**	–83.6	–268.7	–101.8
cyclo-$CuAg_2(\mu_2\text{-H})_3$ **3**	–72.4	–244.8	–77.8
cyclo-$Ag_3(\mu_2\text{-H})_3$ **4**	–62.6	–222.2	–55.2
cyclo-$Cu_4(\mu_2\text{-H})_4$ **5**	–159.1	–423.3	–200.6
cyclo-$Cu_3Ag(\mu_2\text{-H})_4$ **6**	–146.4	–397.8	–175.1
cyclo-$Cu_2Ag_2(\mu_2\text{-H})_4$ **7**	–135.1	–373.6	–150.9
cyclo-$Cu_2Ag_2(\mu_2\text{-H})_4$ **8**	–134.4	–372.9	–150.2
cyclo-$CuAg_3(\mu_2\text{-H})_4$ **9**	–124.5	–350.1	–127.4
cyclo-$Ag_4(\mu_2\text{-H})_4$ **10**	–115.2	–327.9	–105.2
cyclo-$Cu_5(\mu_2\text{-H})_5$ **11**	–208.3	–538.6	–260.3
cyclo-$Cu_4Ag(\mu_2\text{-H})_5$ **12**	–196.5	–513.9	–235.5
cyclo-$Cu_3Ag_2(\mu_2\text{-H})_5$ **13**	–185.5	–490.0	–211.7
cyclo-$Cu_3Ag_2(\mu_2\text{-H})_5$ **14**	–185.0	–489.6	–211.2
cyclo-$Cu_2Ag_3(\mu_2\text{-H})_5$ **15**	–175.1	–466.8	–188.4
cyclo-$Cu_2Ag_3(\mu_2\text{-H})_5$ **16**	–174.5	–466.2	–187.8
cyclo-$CuAg_4(\mu_2\text{-H})_5$ **17**	–165.1	–443.9	–165.6
cyclo-$Ag_5(\mu_2\text{-H})_5$ **18**	–156.0	–421.0	–143.6

[a] $\Delta E_1 = E(M_nH_n) - nE(MH)$. [b] $\Delta E_2 = E(M_nH_n) - [nE(M) + nE(H)]$. [c] $\Delta E_3 = E(M_nH_n) - [nE(M) + (n/2)E(H_2)]$.

Table 2 Selected electronic parameters of the *cyclo*-$Cu_nAg_{3-n}H_n$ (n = 1–3), *cyclo*-$Cu_nAg_{4-n}H_n$ (n = 1–4) and *cyclo*-$Cu_nAg_{5-n}H_n$ (n = 1–5), calculated at the B3LYP/6-31G(d,p) ∪ LANL2DZ(Ag) level

Species	ε_{HOMO}	ε_{LUMO}	$\varepsilon_{(LUMO-HOMO)}$	μ	η	ω
1	−6.24	−1.44	4.80	−3.84	2.40	3.07
2	−6.09	−2.07	4.02	−4.08	2.01	4.14
3	−6.23	−2.03	4.20	−4.13	2.10	4.06
4	−6.70	−1.83	4.87	−4.27	2.44	3.73
5	−6.59	−1.61	4.98	−4.10	2.49	3.38
6	−6.65	−1.79	4.86	−4.22	2.43	3.66
7	−6.67	−1.90	4.77	−4.29	2.39	3.84
8	−6.62	−1.91	4.71	−4.27	2.36	3.85
9	−6.76	−1.98	4.78	−4.37	2.39	4.00
10	−7.21	−2.03	5.18	−4.62	2.59	4.12
11	−6.89	−1.93	4.96	−4.41	2.48	3.92
12	−6.87	−1.92	4.95	−4.40	2.48	3.89
13	−6.86	−1.85	5.01	−4.36	2.51	3.78
14	−6.86	−1.92	4.94	−4.39	2.47	3.90
15	−6.84	−1.83	5.01	−4.34	2.51	3.74
16	−6.91	−1.87	5.04	−4.39	2.52	3.82
17	−6.96	−1.80	5.16	−4.38	2.58	3.72
18	−7.51	−1.74	5.77	−4.63	2.89	3.70

3.4 Vibrational spectra

The most characteristic infrared active vibrational modes of the 3-membered "all-metal" heterocycles along with the normal coordinate vectors (arrows) are shown in Fig. 5.

The harmonic vibrational frequencies and the IR intensities of all the *cyclo*-$Cu_nAg_{3-n}(\mu_2\text{-H})_n$ (n = 1–3), *cyclo*-$Cu_nAg_{4-n}(\mu_2\text{-H})_n$ (n = 1–4) and *cyclo*-$Cu_nAg_{5-n}(\mu_2\text{-H})_n$ (n = 1–5) species are listed in detail in the ESI (Table S1 and Fig. S3–S5†). In general, the most intense bands of all the hydrido-bridged coinage metal heterocycles are related with the hydrido bridges. Thus, the bands in the region of 536–613 cm^{-1} correspond to the out-of-plane bending of the bridging H atoms. In addition, there are bands in the regions of 1011–1192 cm^{-1}, 1201–1295 cm^{-1} and 1320–1442 cm^{-1} corresponding to the in-plane bending of the bridging H atoms. In summary the vibrational modes of the binary copper–silver heterocycles could assist experimentalists in identifying the respective hydrometal heterocycles.

3.5 Electronic spectra

The principal singlet–singlet electronic transitions, excitation energies, wave lengths, oscillator strengths and transition

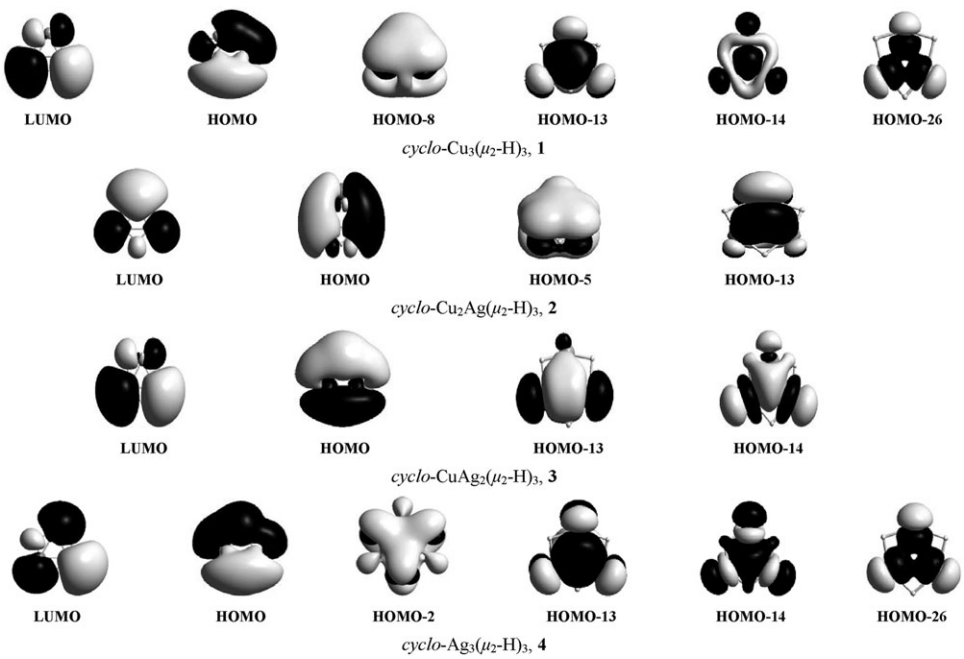

Fig. 4 The most-relevant valence MOs of the *cyclo*-$Cu_nAg_{3-n}(\mu_2\text{-H})_n$ (n = 1–3) species.

View Article Online

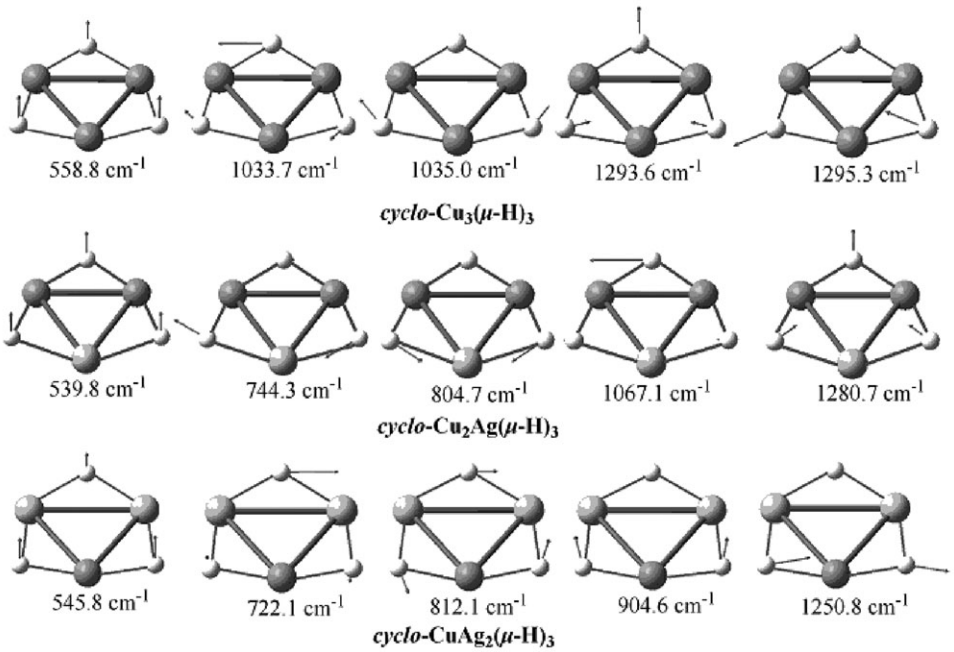

Fig. 5 Infrared active vibrational modes of the 3-membered "all-metal" heterocycles along with the normal coordinate vectors (arrows).

Published on 03 April 2007 on http://pubs.rsc.org | doi:10.1039/B617158C
Downloaded by University of Belgrade on 01 January 2013

Table 3 Principal electronic transitions, excitation energy (E), wavelengths (λ), oscillator strengths (f) and transition dipole moments (m) for the *cyclo*-$Cu_nAg_{3-n}(\mu_2\text{-H})_n$ (n = 1–3), *cyclo*-$Cu_nAg_{4-n}(\mu_2\text{-H})_n$ (n = 1–4) and *cyclo*-$Cu_nAg_{5-n}(\mu_2\text{-H})_n$ (n = 1–5) species computed at the B3LYP/6-31G(d,p) ∪ LANL2DZ(Ag) level

Species	E/eV	λ/nm	f (a.u.)	Excitation[a]	m (a.u.)
1	4.8076	258	0.081	H-4 → L + 2, H-3 → L + 2	0.64
	3.8363	323	0.039	H-1 → L + 1, H → L	0.83
2	5.1691	240	0.109	H-3 → L + 1, H-1 → L + 2, H → L + 3	0.66
	3.9695	312	0.043	H → L + 2	0.93
3	5.3402	232	0.333	H-6 → L, H-1 → L + 3	1.07
	4.7587	261	0.134	H-5 → L, H-3 → L + 2, H → L + 3	1.60
4	5.2994	234	0.314	H-1 → Lv3, H → Lv3	1.01
	4.3133	287	0.107	H-1 → L, H → L + 1	1.55
5	4.3457	285	0.215	H → L + 2, H-8 → L	1.42
6	4.0269	308	0.105	H → L	0.34
7	4.6584	266	0.155	H-1 → L + 2, H-4 → L	1.17
	5.2899	234	0.293	H-9 → L + 1, H-1 → L + 2	1.34
8	4.5428	272	0.102	H-4 → L, H → L + 2	0.96
	3.9882	311	0.175	H → L	1.50
	5.3665	231	0.240	H-4 → L + 2, H-1 → L + 2, H → L + 3	1.06
9	4.6470	267	0.146	H → L + 2, H-2 → L	1.13
	4.0726	304	0.112	H → L	1.35
	6.2506	198	0.037	H-6 → L, H-3 → L + 1	0.97
10	5.3077	234	0.442	H → L + 2	1.84
	4.6105	269	0.114	H-1 → L	0.49
11	4.1311	300	0.133	H → L	1.15
12	4.1907	296	0.148	H-2 → L	1.20
	4.8441	256	0.125	H-1 → L + 2, H-6 → L + 1	1.02
13	4.9820	249	0.021	H-2 → L + 2, H-11 → L	0.31
	4.0856	303	0.010	H → L	0.41
14	4.8424	256	0.148	H → L + 3, H-1 → L + 2	1.30
	4.2138	294	0.174	H-1 → L	1.12
15	4.8551	255	0.141	H → L + 3, H-1 → L + 2	0.95
	4.3593	284	0.096	H-1 → L, H-6 → L	1.09
16	4.8487	256	0.109	H-1 → L + 2, H → L + 3	1.22
	4.2333	293	0.154	H → L	0.96
	5.5284	224	0.210	H-3 → L + 2	0.95
17	4.9765	249	0.073	H-1 → L, H-5 → L	0.77
	4.3235	287	0.095	H → L	1.25
18	5.7336	216	0.386	H-3 → L + 2, H-2 → L + 3	1.66

[a] H and L stand for HOMO and LUMO, respectively.

 This journal is © the Royal Society of Chemistry and the Centre National de la Recherche Scientifique 2007

Published on 03 April 2007 on http://pubs.rsc.org | doi:10.1039/B617158C
Downloaded by University of Belgrade on 01 January 2013

dipole moments for the *cyclo*-$Cu_nAg_{3-n}(\mu_2\text{-}H)_n$ (n = 1–3), *cyclo*-$Cu_nAg_{4-n}(\mu_2\text{-}H)_n$ (n = 1–4) and *cyclo*-$Cu_nAg_{5-n}(\mu_2\text{-}H)_n$ (n = 1–5) species calculated with the TD-DFT at the B3LYP/6-31G(d,p) ∪ LANL2DZ(Ag) level, are given in Table 3.

The TD-DFT computed electronic absorption spectra of hydrido-bridged binary coinage metal heterocycles under consideration are given in Fig. 6.

Inspection of Table 3 and Fig. 6 reveals that all excitations occur in the ultraviolet region. The electronic spectra of the triangular hydrido-bridged coinage metal heterocycles are dominated by two absorption bands *i.e.* one strong band in the region of 232–273 nm and another weaker band in the region of 261–323 nm. In general, a red shift is observed upon replacing Cu atoms with Ag atoms in the ring of the *cyclo*-$Cu_nAg_{3-n}(\mu_2\text{-}H)_n$ (n = 1–3) metal clusters. On the other hand, the electronic spectra of the tetranuclear *cyclo*-$Cu_nAg_{4-n}(\mu_2\text{-}H)_n$ (n = 1–4) species fall into two categories: (a) species **5–7** with electronic spectra characterized mainly by one strong band in the region 266–308 nm and (b) species **8–10** whose electronic spectra are characterized by one strong band in the region 230–235 nm and two weaker bands. Noteworthy also is the presence of a shoulder in the electronic spectra of species **6** and **7** in the region of 240–260 nm in contrast to the electronic spectrum of **5** where no such shoulder exists.

The electronic spectra of the pentanuclear *cyclo*-$Cu_nAg_{5-n}(\mu_2\text{-}H)_n$ (n = 1–5) species are characterized by two strong bands with the exception of the homonuclear *cyclo*-$Cu_5(\mu_2\text{-}H)_5$, **11**, and $Ag_5(\mu_2\text{-}H)_5$, **18**, metal clusters whose spectra exhibit only one strong band. Finally, in the electronic spectra of the *cyclo*-$CuAg_4(\mu_2\text{-}H)_5$, **17** species three instead of two characteristic bands exist.

3.6 NMR spectra and aromaticity

In order to check if the hydrido-bridged coinage metal heterocycles are aromatic or antiaromatic molecules we have estimated the nucleus independent chemical shifts, NICS(0) and NICS(1) given in Table 4. The NICS values were proposed by Schleyer *et al.*[29] as a magnetic criterion of aromaticity. Perusal of Table 4 reveals that the 3- and 4-membered hydrido-bridged coinage metal heterocycles posses significant aromatic character (NICS(0) values in the range of −5.0 to −14.7 ppm), while the 5-membered hydrido-bridged coinage metal heterocycles exhibit negligible aromaticity and therefore could be considered as non aromatic "all-metal" heterocycles. The absolute ^{63}Cu and ^{109}Ag isotropic shielding tensor elements are consistent with the charge density distribution on the metal atoms. The Ag atoms in the ring introduce a shielding on the Cu atoms which increases significantly upon increasing the Ag hetero-atoms in the rings. On the other hand, the ^{109}Ag isotropic shielding tensor elements seem to be unaffected by substitution of Ag atoms of the rings by Cu hetero-atoms. The ^{109}Ag isotropic shielding tensor elements are found in the range of 259–267 ppm. The ^{1}H NMR chemical shifts (δ, ppm) computed from the difference between the shielding of the reference TMS standard and the shielding of the molecule of interest, $\delta = \sigma_{ref} - \sigma$ are also given in Table 4.

It can be seen that the hydride ligands of the species that exhibit remarkable aromatic character quantified by the NICS(0) and NICS(1) values are paramagnetically deshielded as it is the case for the protons in the aromatic organic analogues.

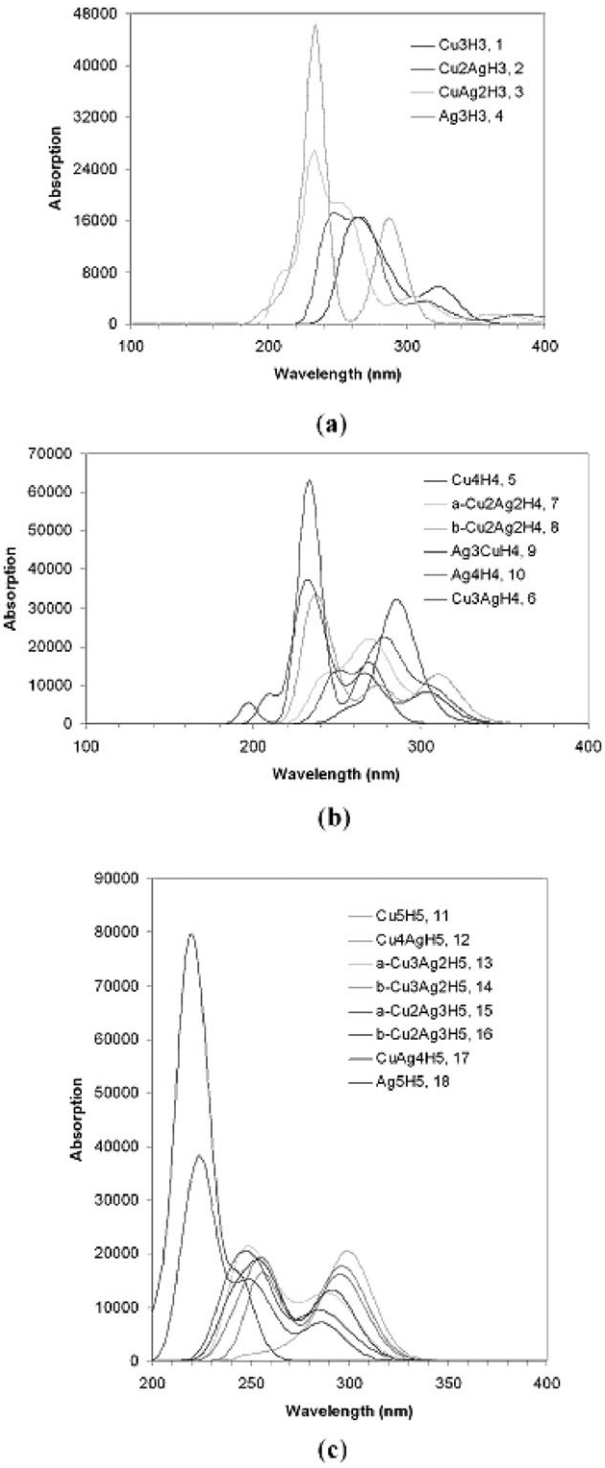

Fig. 6 Electronic absorption spectra of hydrido-bridged binary coinage metal heterocycles computed by TD-DFT at the B3LYP/6-31G(d,p) ∪ LANL2DZ(Ag) level.

View Article Online

Table 4 ^{65}Cu, ^{109}Ag and ^{1}H isotropic shielding tensor elements (σ^{iso}, ppm) and the NICS(0) and NICS(1) values (ppm) of binary coinage metal heterocycles, calculated at the GIAO/B3LYP/6-31G(d,p) ∪ LANL2DZ(Ag)//B3LYP/6-31G(d,p) ∪ LANL2DZ(Ag) level

Species	σ^{iso}(^{65}Cu)	σ^{iso}(^{109}Ag)	σ^{iso}(^{1}H)	δ(^{1}H)[c]	NICS(0)	NICS(1)
cyclo-$Cu_3(\mu\text{-}H)_3$, **1**	45.6		29.4	2.2	−14.7	−4.2
cyclo-$Cu_2Ag(\mu\text{-}H)_3$, **2**	61.4	263.4	28.3 (30.2)[b]	3.3 (1.4)	−12.1	−4.3
cyclo-$CuAg_2(\mu\text{-}H)_3$, **3**	73.4	261.6	26.9 (*28.9*)	4.7 (*2.7*)	−10.3	−4.0
cyclo-$Ag_3(\mu\text{-}H)_3$, **4**		261.4	(*27.4*)	(*4.2*)	−9.2	−3.9
cyclo-$Cu_4(\mu\text{-}H)_4$, **5**	69.1		31.9	−0.3	−8.6	−4.2
cyclo-$Cu_3Ag(\mu\text{-}H)_4$, **6**	104.4 (76.5)[a]	259.2	32.0 (30.6)	−0.4 (1.0)	−7.5	−3.3
cyclo-$Cu_2Ag_2(\mu\text{-}H)_4$, **7**	122.0	260.8	32.1 (30.7, *29.4*)	−0.5 (0.9, *2.2*)	−6.3	−2.8
cyclo-$Cu_2Ag_2(\mu\text{-}H)_4$, **8**	140.3	259.7	(30.7)	(0.9)	−7.0	−3.4
cyclo-$CuAg_3(\mu\text{-}H)_4$, **9**	162.4	261.9 (261.7)	(30.8, *29.6*)	(0.8, *2.0*)	−5.6	−2.7
cyclo-$Ag_4(\mu\text{-}H)_4$, **10**		263.2	(*29.7*)	(*1.5*)	−5.0	−2.5
cyclo-$Cu_5(\mu\text{-}H)_5$, **11**	86.4–91.9		32.5	−0.9	−2.8	−1.3
cyclo-$Cu_4Ag(\mu\text{-}H)_5$, **12**	100.8 (130.4)	263.3	32.7 (31.2)	−1.1 (0.4)	−2.6	−1.3
cyclo-$Cu_3Ag_2(\mu\text{-}H)_5$, **13**	114.4 (144.4)	264.2	32.6 (31.1, *30.3*)	−1.0 (0.5, *1.3*)	−2.0	−0.8
cyclo-$Cu_3Ag_2(\mu\text{-}H)_5$, **14**	(141.0, *157.5*)	264.0	32.5 (31.5)	−0.9 (0.1)	−2.5	−1.2
cyclo-$Cu_2Ag_3(\mu\text{-}H)_5$, **15**	155.1	265.2	32.5 (31.4, *30.3*)	−0.9 (0.2, *1.3*)	−1.7	−0.7
cyclo-$Cu_2Ag_3(\mu\text{-}H)_5$, **16**	(171.4)	264.9	(31.4, *30.5*)	(0.2, *1.1*)	−2.2	−1.0
cyclo-$CuAg_4(\mu\text{-}H)_5$, **17**	(184.5)	266.0	(31.3, *30.4*)	(0.3, *1.2*)	−1.6	−0.7
cyclo-$Ag_5(\mu\text{-}H)_5$, **18**		267.1	(*30.4*)	(*1.2*)	−1.3	−0.6

[a] Figures in parentheses are the σ^{iso} values of Cu atoms bonded simultaneously to Cu and Ag atoms (plain) or to two Ag atoms (italics). [b] Figures in parentheses are the σ^{iso} values of H atoms bonded simultaneously to Cu and Ag atoms (plain) or to two Ag atoms (italics). [c] The ^{1}H chemical shift (δ, ppm) is equal to the difference between the ^{1}H shielding of the TMS external reference standard (σ^{iso} = 31.6 ppm, σ^{aniso} = 9.2 ppm) and the ^{1}H shielding of the molecule.

Published on 03 April 2007 on http://pubs.rsc.org | doi:10.1039/B617158C
Downloaded by University of Belgrade on 01 January 2013

4. Conclusions

In this paper we have reported a comprehensive DFT study of the structural, energetic, spectroscopic (IR, NMR, UV-Vis), electronic and bonding properties of a new series of model "all-metal" binary coinage metal heterocycles. These novel classes of inorganic compounds can be considered as the archetypes for the development of whole classes of new "all-metal" inorganic aromatic heterocyclic species (substituted derivatives) resulting from substitution of the H atoms by other groups, such as alkyls (R) and aryls (Ar), halides (X), amido (NR_2), hydroxide (OH) and alkoxides (OR) *etc*.

The results can be summarized as follows:

All *cyclo*-$Cu_nAg_{3-n}(\mu_2\text{-}H)_n$ (n = 1–3), *cyclo*-$Cu_nAg_{4-n}(\mu_2\text{-}H)_n$ (n = 1–4) and *cyclo*-$Cu_nAg_{5-n}(\mu_2\text{-}H)_n$ (n = 1–5) species predicted to be stable molecules have a structure analogous to the corresponding heterocyclic aromatic organic analogues, which is characterized by perfect planarity. The planar "all-metal" binary coinage metal heterocycles are predicted to be strongly bound molecules with respect to their dissociation either to the MH monomers or to free M and H atoms in their ground states. The computed total binding energies of the MH monomers to form the *cyclo*-M_nH_n species are found in the range of 62.6–208.3 kcal mol^{-1}.

Based on the predicted stability of the "all-metal" binary coinage metal heterocycles with respect either to the constituent atoms or to the standard states of their elements one would expect such species to be formed in MS of binary Cu–Ag vapor sputtered with hydrogen or by the normal spectroscopic approach of deposition of the Cu–Ag alloy in a hydrogen matrix.

The bonding of *cyclo*-$Cu_nAg_{3-n}(\mu_2\text{-}H)_n$ (n = 1–3), *cyclo*-$Cu_nAg_{4-n}(\mu_2\text{-}H)_n$ (n = 1–4) and *cyclo*-$Cu_nAg_{5-n}(\mu_2\text{-}H)_n$ (n = 1–5) species is characterized by a common ring-shaped electron density, more commonly seen in organic molecules, which is constructed by highly delocalized σ-, π- and δ-type MOs.

We have also reported the computed spectroscopic properties (IR, NMR, UV-Vis and photoelectron) of the "all-metal" binary coinage metal heterocycles in order to assist in identifying the respective aromatic "all-metal" compounds and to help with future laboratory studies. A complete assignment of the most characteristic infrared absorption bands is given, while the aromaticity of the "all-metal" heterocycles was estimated by making use of several criteria for aromaticity, such as the NICS(0) and NICS(1) parameters and the electrophilicity index ω. The principal singlet–singlet electronic transitions, excitation energies and oscillator strengths of the "all-metal" aromatic binary coinage metal heterocycles were calculated with the TD-DFT using the B3LYP functionals and the assignment of the electronic transitions is given.

References

1 W. Ekardt, *Metal Clusters*, John Wiley, NY, 1999.
2 V. W.-W. Yam, W. K.-M. Fung and K.-K. Cheung, *J. Cluster Sci.*, 1999, **10**, 37.
3 M. Niemeyer, *Organometallics*, 1998, **17**, 4649, and references therein.
4 H. Eriksson and M. Håkansson, *Organometallics*, 1997, **16**, 4243.
5 J. A. J. Jarvis, B. T. Kilbourn, R. Pearce and M. F. Lappert, *J. Chem. Soc., Chem. Commun.*, 1973, 475.
6 V. W.-W. Yam and K. K.-Y. Lo, *Chem. Soc. Rev.*, 1999, **28**, 323.
7 J. P. Fackler, Jr, *Inorg. Chem.*, 2002, **41**, 6959, and references therein.
8 M. Bardaji and A. Laguna, *Eur. J. Inorg. Chem.*, 2003, 3069, and references therein.
9 (*a*) F. Scherbaum, A. Grohmann, B. Huber, C. Krüger and H. Schmidbaur, *Angew. Chem., Int. Ed. Engl.*, 1988, **27**, 1544; (*b*) H. Schmidbaur, *Gold Bull.*, 2000, **33**, p. 3; (*c*) H. Schmidbaur, *Nature*, 2001, **413**, 31.
10 P. Pyykkö, *Chem. Rev.*, 1997, **97**, 597.
11 H. L. Hermann, G. Boche and P. Schwerdtfeger, *Chem.–Eur. J.*, 2001, **7**, 5333.

 This journal is © the Royal Society of Chemistry and the Centre National de la Recherche Scientifique 2007

View Article Online

12 J.-P. Zhang, Y.-B. Wang, X.-C. Huang, Y.-Y. Lin and X.-M. Chen, *Chem.–Eur. J.*, 2005, **11**, 552.
13 A. C. Tsipis and C. A. Tsipis, *J. Am. Chem. Soc.*, 2003, **125**, 1136.
14 A. C. Tsipis, E. E. Karagiannis, P. F. Kladou and C. A. Tsipis, *J. Am. Chem. Soc.*, 2004, **126**, 12916.
15 C. S. Wannere, C. Corminboeuf, Z.-X. Wang, M. D. Wodrich, R. B. King and P. v. R. Schleyer, *J. Am. Chem. Soc.*, 2005, **127**, 5701.
16 Z. Chen, C. S. Wannere, C. Corminboeuf, R. Puchta and P. v. R. Schleyer, *Chem. Rev.*, 2005, **105**, 3842.
17 C. A. Tsipis, *Coord. Chem. Rev.*, 2005, **249**, 2740.
18 A. I. Boldyrev and L.-S. Wang, *Chem. Rev.*, 2005, **105**, 3716.
19 M. A. Omary, M. A. Rawashdeh-Omary, M. W. Alexander Gonser, O. Elbjeirami, T. Grimes and T. R. Cundari, *Inorg. Chem.*, 2005, **44**, 8200, and references therein.
20 R. Pattacini, L. Barbieri, A. Stercoli, D. Cauzzi, C. Graiff, M. Lanfranchi, A. Tiripicchio and L. Elviri, *J. Am. Chem. Soc.*, 2006, **128**, 866.
21 A. D. Becke, *J. Chem. Phys.*, 1992, **96**, 2155.
22 A. D. Becke, *J. Chem. Phys.*, 1993, **98**, 5648.
23 C. Lee, W. Yang and R. G. Parr, *Phys. Rev. B*, 1988, **37**, 785.
24 H. B. Schlegel, *J. Comput. Chem.*, 1982, **3**, 214.
25 A. E. Reed, L. A. Curtiss and F. Weinhold, *Chem. Rev.*, 1988, **88**, 899–926.
26 F. Weinhold, in *The Encyclopedia of Computational Chemistry*, ed. P. v. R. Schleyer, John Wiley & Sons, Chichester, 1998, pp. 1792–1811.
27 R. Ditchfield, *Mol. Phys.*, 1974, **27**, 789.
28 J. Gauss, *J. Chem. Phys.*, 1993, **99**, 3629.
29 P. v. R. Schleyer, C. Maerker, A. Dransfeld, H. Jiao and N. J. Hommes, *J. Am. Chem. Soc.*, 1996, **118**, 6317.
30 S. J. A. van Gisbergen, F. Kootstra, P. R. T. Schipper, O. V. Gritsenko, J. G. Snijders and E. J Baerends, *Phys. Rev. A*, 1998, **57**, 1556.
31 C. Jamorski, M. E. Casida and D. R. Salahud, *J. Chem. Phys.*, 1996, **104**, 5134.
32 R. Bauernschmitt and R. Ahlrichs, *Chem. Phys. Lett.*, 1996, **256**, 454.
33 M. Frisch G. W. Trucks, H. B. Schlegel, G. E. Scuseria, M. A. Robb, J. R. Cheeseman, J. A. Montgomery, Jr, T. Vreven, K. N. Kudin, J. C. Burant, J. M. Millam, S. S. Iyengar, J. Tomasi, V. Barone, B. Mennucci, M. Cossi, G. Scalmani, N. Rega, G. A. Petersson, H. Nakatsuji, M. Hada, M. Ehara, K. Toyota, R. Fukuda, J. Hasegawa, M. Ishida, T. Nakajima, Y. Honda, O. Kitao, H. Nakai, M. Klene, X. Li, J. E. Knox, H. P. Hratchian, J. B. Cross, C. Adamo, J. Jaramillo, R. Gomperts, R. E. Stratmann, O. Yazyev, A. J. Austin, R. Cammi, C. Pomelli, J. W. Ochterski, P. Y. Ayala, K. Morokuma, G. A. Voth, P. Salvador, J. J. Dannenberg, V. G. Zakrzewski, S. Dapprich, A. D. Daniels, M. C. Strain, O. Farkas, D. K. Malick, A. D. Rabuck, K. Raghavachari, J. B. Foresman, J. V. Ortiz, Q. Cui, A. G. Baboul, S. Clifford, J. Cioslowski, B. B. Stefanov, G. Liu, A. Liashenko, P. Piskorz, I. Komaromi, R. L. Martin, D. J. Fox, T. Keith, M. A. Al-Laham, C. Y. Peng, A. Nanayakkara, M. Challacombe, P. M. W. Gill, B. Johnson, W. Chen, M. W. Wong, C. Gonzalez and J. A. Pople, *GAUSSIAN 03, (Revision B.02)*, Gaussian, Inc., Pittsburgh, PA, 2003.
34 A. Bondi, *J. Phys. Chem.*, 1964, **68**, 441.
35 R. G. Parr, L. v. Szentpály and S. Liu, *J. Am. Chem. Soc.*, 1999, **121**, 1922.
36 P. Geerlings, F. De Proft and W. Langenaeker, *Chem. Rev.*, 2003, **103**, 1793.

Published on 03 April 2007 on http://pubs.rsc.org | doi:10.1039/B617158C
Downloaded by University of Belgrade on 01 January 2013